PERGAMON International Journal of Mechanical Sciences 43 (2001) 1195–1208

International Journal of MECHANICAL SCIENCES

www.elsevier.com/locate/ijmecsci

Chaotic dynamic analysis of viscoelastic plates

Y.X. Sun*, S.Y. Zhang

Laboratory for Nonlinear Mechanics of Continuous Media, Institute of Mechanics, Chinese Academy of Sciences, Beijing, 100080, People's Republic of China

Received 7 June 1999; received in revised form 24 July 2000

Abstract

The dynamic buckling of viscoelastic plates with large deflection is investigated in this paper by using chaotic and fractal theory. The material behavior is given in terms of the Boltzmann superposition principle. In order to obtain accurate computation results, the nonlinear integro-differential dynamic equation is changed into an autonomic four-dimensional dynamical system. The numerical time integrations of equations are performed by using the fourth-order Runge–Kutta method. And the Lyapunov exponent spectrum, the fractal dimension of strange attractors and the time evolution of deflection are obtained. The influence of geometry nonlinearity and viscoelastic parameter on the dynamic buckling of viscoelastic plates is discussed.

Keywords: Viscoelastic plates; Dynamic buckling; Chaos and fractal; Geometry nonlinearity

1. Introduction

The composite materials developed today are being used increasingly for plate and shell structures such as aerospace vehicles, rocket engines, turbine blades, nuclear reactors, etc. The accurate prediction of their instability behavior plays a crucial role in their reliable and lightweight structural design. Due to the elevated temperatures experienced by these structures, their constituent materials exhibit a time-dependent properties that could be modeled by a viscoelastic constitutive law. The problem of the dynamical stability of elastic structures was extensively investigated by Bolotin [1] and further results were given, for example, by Evan-Iwanowski [2,3] in a review paper and a monograph, respectively. When the structure is made of viscoelastic material, the problem

* Corresponding author now at: Dept. 8th. 831, Beijing Institute of Technology, Beijing 100081, People's Republic of China.

E-mail address: sunyx99@sohu.com (Y.X. Sun).

0020-7403/01/$ - see front matter
PII: S0020-7403(00)00062-X

Nomenclature

a	plate dimension in x direction
A	constant in Eq. (3)
b	plate dimension in y direction
B	constant in Eq. (3)
D	plate's cylindrical bending stiffness
D_0	fractal dimension of the strange attractor
f_{mn}	displacement amplitude
$\bar{f}_{mn}$	dimensionless quantities in Eq. (13)
h	plate thickness
$L(\ )$	differential operator, expressed by Eq. (7)
l	dimension of square plate
LE_i	Lyapunov exponent
N	the Euler critical load
$N_x(t)$	in-plane load
N_{xs}	static load component
N_{xd}	dynamic load component
q_1, q_2, q_3	constants in Eq. (16)
$R^*[\ ]$	integral operator, expressed by Eq. (4)
R_1, R_2, R_3, R_4	parameters in Eqs. (27) and (31)
SJF	summation in Eq. (29)
Z	integration expressed by Eq. (18)
u, v, w	displacement in x, y, and z directions
$Y(t)$	time-dependent relaxation function
$Y(0)$	initial Young's modulus of the material;
$Y(\infty)$	longtime modulus of the material
$t_r = \frac{1}{\alpha}$	relaxation time

Greek Letters

α	material coefficient in Eq. (3)
Δt	time incremental.
$\varepsilon_x, \varepsilon_y, \gamma_{xy}$	components of strain
$\sigma_x, \sigma_y, \tau_{xy}$	components of stress
η	the excitation parameter
η_c	critical value of the excitation parameter
θ	load frequency
λ	ratio of plate dimension in x direction to dimension in y direction, a/b
μ	Poisson's ratio
ρ	material density
ϕ	stress function
ω	natural frequency of lateral vibration of unloaded plates
Ω	natural frequency of lateral vibration of loaded plates

becomes much more complicated since the equation of motion turns out to be an integro-differential one, rather than an ordinary differential equation as in the elastic case.

The dynamic stability of viscoelastic homogeneous plates studied based on the small deflections theory and the concept of the Lyapunov exponents was investigated by Aboudi et al. [4] and Touati et al. [5] . This procedure was used also by Cederbaum et al. [6] to investigate the dynamic stability of shear deformable viscoelastic laminated plates. The dynamic stability of viscoelastic column [7], viscoelastic homogeneous plates [8] and viscoelastic orthotropic laminated plates [9] was investigated by Cederbaum et al. by using the multiple-scales method.

The research activity devoted to stability of viscoelastic plates with large deflection appears to be scarce. Badalov et al. [10] investigated dynamic stability of viscoelastic plates subjected to an in-plane constant rate loading. Zhu Yuanyuan and Cheng Changjun [11] analyzed the stability of viscoelastic rectangular plates from the point of view of dynamical system with ignoring the inertia terms. Touati and Cederbaum [12] analyzed the dynamic stability of nonlinear viscoelastic plates.

In the present paper, the dynamic stability of viscoelastic plates with large deflection is investigated. We calculate the Lyapunov exponent spectrum, the fractal dimension of strange attractors and the time evolution of deflection. The influence of geometry nonlinearity and viscoelastic parameter on the dynamic buckling of viscoelastic plates is discussed.

2. Problem equations

The problem of the simply-supported viscoelastic plates subjected to an in-plane periodic load (as shown in Fig. 1) is considered.

For the plate with large deflection, the von Karman nonlinear strain–deflection relations are given as [10]

$$\varepsilon_x = \frac{\partial u}{\partial x} + \frac{1}{2}\left(\frac{\partial w}{\partial x}\right)^2,$$
$$\varepsilon_y = \frac{\partial v}{\partial y} + \frac{1}{2}\left(\frac{\partial w}{\partial y}\right)^2, \tag{1}$$
$$\gamma_{xy} = \frac{\partial u}{\partial y} + \frac{\partial v}{\partial x} + \frac{\partial w}{\partial x}\frac{\partial w}{\partial y}.$$

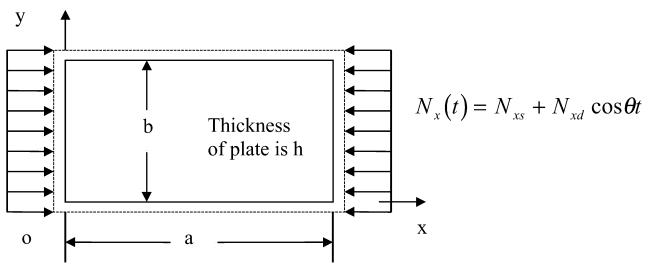

Fig. 1. Scheme of a plate subjected to in-plane loading.

The physical relations between the stresses in the middle surface $\sigma_x, \sigma_y, \tau_{xy}$ and the strains ε_x, ε_y, γ_{xy} are given as [10]:

$$\sigma_x = \frac{Y(0)}{1-\mu^2}(1-R^*)(\varepsilon_x + \mu\varepsilon_y),$$

$$\sigma_y = \frac{Y(0)}{1-\mu^2}(1-R^*)(\varepsilon_y + \mu\varepsilon_x), \tag{2}$$

$$\tau_{xy} = \frac{Y(0)}{2(1+\mu)}(1-R^*)\gamma_{xy},$$

where μ is Poisson's ratio that can be assumed to be time independent [13].

$Y(t)$ is a time-dependent relaxation function. In this paper, the viscoelastic material is modeled as the standard linear solid-type material, where the relaxation function is given by

$$Y(t) = A + B\mathrm{e}^{-\alpha t} \tag{3}$$

where A, B, α are appropriate parameters.

$Y(0) = A + B$, is the initial Young's modulus of the material; $Y(\infty) = A$, is the longtime modulus, $t_r = 1/\alpha$ is the relaxation time and R^* is an integral operator having the following expression:

$$R^*[f(t)] = \alpha\frac{Y(0)-Y(\infty)}{Y(0)}\int_0^t f(\tau)\mathrm{e}^{-\alpha(t-\tau)}\,\mathrm{d}\tau. \tag{4}$$

Inserting Eqs. (1) and (2) into the equilibrium equations (5) and compatibility equation (6) [10]:

$$\frac{\partial\sigma_x}{\partial x} + \frac{\partial\tau_{xy}}{\partial y} = 0,$$

$$\frac{\partial\tau_{xy}}{\partial x} + \frac{\partial\sigma_y}{\partial y} = 0,$$

$$-\frac{D}{h}(1-R^*)\nabla^4 w + \frac{\partial}{\partial x}\left(\sigma_x\frac{\partial w}{\partial x} + \tau_{xy}\frac{\partial w}{\partial y}\right) + \frac{\partial}{\partial y}\left(\tau_{xy}\frac{\partial w}{\partial x} + \sigma_y\frac{\partial w}{\partial y}\right) - \rho\frac{\partial^2 w}{\partial t^2} = 0, \tag{5}$$

$$\frac{\partial^2\varepsilon_x}{\partial y^2} + \frac{\partial^2\varepsilon_y}{\partial x^2} - \frac{\partial^2\gamma_{xy}}{\partial x\partial y} = -\frac{1}{2}L(w,w), \tag{6}$$

where

$$L(f_1,f_2) = \frac{\partial^2 f_1}{\partial x^2}\frac{\partial^2 f_2}{\partial y^2} + \frac{\partial^2 f_1}{\partial y^2}\frac{\partial^2 f_2}{\partial x^2} - 2\frac{\partial^2 f_1}{\partial x\partial y}\frac{\partial^2 f_2}{\partial x\partial y} \tag{7}$$

and referring to Ref. [14], the following system of equations for determining the deflection w and stress function ϕ are obtained [10]:

$$\frac{D}{h}(1-R^*)\nabla^4 w = L(w,\phi) - \rho\frac{\partial^2 w}{\partial t^2},$$

$$\frac{1}{Y(0)}\nabla^4\phi = -\frac{1}{2}(1-R^*)L(w,w), \tag{8}$$

where, $D = Y(0)h^3/12(1-\mu^2)$ is the plate's cylindrical bending stiffness and h is the thickness.

The boundary conditions may be expressed as follows:

$$w = \frac{\partial^2 w}{\partial x^2} + \mu\frac{\partial^2 w}{\partial y^2} = 0 \quad \text{along } x = 0, a,$$

$$w = \frac{\partial^2 w}{\partial y^2} + \mu\frac{\partial^2 w}{\partial x^2} = 0 \quad \text{along } y = 0, b,$$

$$\frac{\partial^2\phi}{\partial y^2} = -\frac{N_x(t)}{h}, \quad \frac{\partial^2\phi}{\partial x\partial y} = 0 \quad \text{along } x = 0, a,$$

$$\frac{\partial^2\phi}{\partial x^2} = 0, \quad \frac{\partial^2\phi}{\partial x\partial y} = 0 \quad \text{along } y = 0, b.$$

Considering that the plate is hinged at its boundaries, the solution of Eq. (8), which satisfies the boundary conditions of the problem, can be expressed as

$$w(x,y,t) = \sum_{m=1}^{\infty}\sum_{n=1}^{\infty} f_{mn}(t)\sin\frac{m\pi x}{a}\sin\frac{n\pi y}{b} \tag{9}$$

Substituting Eq. (9) into the second equation of Eq. (8) at a fixed pair of $\{m,n\}$, we obtain the stress function

$$\phi = \frac{Y(0)}{32}(1-R^*)f_{mn}^2\left[\left(\frac{n\lambda}{m}\right)^2\cos\frac{2m\pi x}{a} + \left(\frac{m}{n\lambda}\right)^2\cos\frac{2n\pi y}{b}\right] - \frac{N_x(t)y^2}{2h}, \tag{10}$$

where

$$\lambda = \frac{a}{b}. \tag{11}$$

Now inserting Eqs. (9) and (10) into the first equation of Eq. (8) and using the Bubnov–Galerkin method to determine f_{mn}, we obtain the following system of nonlinear integro-differential equation:

$$\frac{\rho b^4}{Y(0)h^2\pi^2}\ddot{f}_{mn} - \left(\frac{m}{\lambda}\right)^2\frac{N_x(t)}{hY(0)}\left(\frac{b}{h}\right)^2 f_{mn} + \frac{\pi^2}{12(1-\mu^2)}\left[\left(\frac{m}{\lambda}\right)^2 + n^2\right]^2(1-R^*)f_{mn}$$
$$+ \frac{\pi^2}{16h^2}\left[\left(\frac{m}{\lambda}\right)^4 + n^4\right]f_{mn}(1-R^*)f_{mn}^2 = 0, \tag{12}$$

where the "$*$" denotes differentiation with respect to t.

Introducing the following dimensionless quantities into Eq. (12)

$$\bar{f}_{mn} = \frac{f_{mn}}{h}. \tag{13}$$

For the sake of concise, " − " and "*mn*" will be omitted later on.

In the following, the main stability region is investigated, for which m and n are simply equal to 1.

Letting $a = b = l$ (a square plate). Then, Eq. (12) is rewritten in the form

$$\ddot{f} + \Omega^2(1 - 2\eta\cos\theta t)f - \omega^2 R^* f + \frac{3(1-\mu^2)}{8}\omega^2 f(1 - R^*)f^2 = 0, \tag{14}$$

where

$$\omega^2 = \frac{h^2 Y(0)}{3(1-\mu^2)\rho}\left(\frac{\pi}{l}\right)^4, \quad N = \frac{\pi^2 h^3 Y(0)}{3(1-\mu^2)l^2},$$

$$\Omega^2 = \omega^2\left(1 - \frac{N_{xs}}{N}\right), \quad \eta = \frac{N_{xd}}{2(N - N_{xs})}.$$

Here, ω and Ω represent the natural frequency of lateral vibration of unloaded and loaded plates, respectively, N is the Euler critical load, η is the excitation parameter.

By using Eq. (4), Eq. (14) is rewritten as

$$\ddot{f} + \Omega^2(1 - 2\eta\cos\theta t)f - q_2 q_3 \int_0^t \mathrm{e}^{-\alpha(t-\tau)} f \,\mathrm{d}\tau + q_1 q_3 f^3 - q_1 q_2 q_3 f \int_0^t \mathrm{e}^{-\alpha(t-\tau)} f^2 \,\mathrm{d}\tau = 0 \tag{15}$$

where

$$q_1 = \frac{3(1-\mu^2)}{8}, \quad q_2 = \frac{Y(0) - Y(\infty)}{Y(0)}\alpha, \quad q_3 = \omega^2. \tag{16}$$

Multiplying Eq. (15) by $\mathrm{e}^{\alpha t}$, and then differentiating it with respect to t, Eq. (15) can be written as

$$\begin{aligned} &\alpha\mathrm{e}^{\alpha t}\dddot{f} + \mathrm{e}^{\alpha t}\ddot{f} + \alpha\mathrm{e}^{\alpha t}\Omega^2(1 - 2\eta\cos\theta t)f + 2\eta\theta\Omega^2\sin\theta t\mathrm{e}^{\alpha t}f \\ &\quad + \mathrm{e}^{\alpha t}\Omega^2(1 - 2\eta\cos\theta t)\dot{f} - q_2 q_3 \mathrm{e}^{\alpha t} f + 3q_1 q_3 \mathrm{e}^{\alpha t} f^2 \dot{f} + q_1 q_3 \alpha \mathrm{e}^{\alpha t} f^3 \\ &\quad - q_1 q_2 q_3 \dot{f} Z - q_1 q_2 q_3 \mathrm{e}^{\alpha t} f^3 = 0, \end{aligned} \tag{17}$$

where

$$Z = \int_0^t \mathrm{e}^{\alpha\tau} f^2 \,\mathrm{d}\tau. \tag{18}$$

For the case of $\alpha = 0$ and neglecting nonlinear terms in Eq. (15), one obtains the well-known linear Mathieu equation, which was extensively investigated, for example, by McLachlan [15]

$$\frac{\mathrm{d}^2 f}{\mathrm{d}t^2} + \Omega^2(1 - 2\eta\cos\theta t)f = 0. \tag{19}$$

When neglecting nonlinear terms in Eq. (15), and $\alpha \neq 0$, we have the following equation which describes the motion of a viscoelastic plate with small deflections:

$$\ddot{f} + \Omega^2(1 - 2\eta\cos\theta t)f - q_2 q_3 \int_0^t e^{-\alpha(t-\tau)} f \, d\tau = 0. \tag{20}$$

Multiplying Eq. (20) by $e^{\alpha t}$, and then differentiating it with respect to t, Eq. (20) can be rewritten as

$$\alpha e^{\alpha t}\ddot{f} + e^{\alpha t}\dddot{f} + e^{\alpha t}\Omega^2(1 - 2\eta\cos\theta t)\dot{f} + \alpha e^{\alpha t}\Omega^2(1 - 2\eta\cos\theta t)f$$

$$+ 2\eta\theta\sin\theta t e^{\alpha t}\Omega^2 f - q_2 q_3 e^{\alpha t} f = 0. \tag{21}$$

The stability of this equation was investigated analytically [7,8], where the expression for the critical (minimum) value of the excitation parameter, η_c, at which instability may occur, was obtained. For the case of the standard linear solid model it is

$$\eta_c = \frac{2\alpha B}{\theta(A + B)} = \frac{2\alpha(Y(0) - Y(\infty))}{\theta Y(0)} \tag{22}$$

and will be used later on.

3. Lyapunov exponents and dimension

Interest here is in the stability of the unperturbed equilibrium of the viscoelastic plate. To this end the integro-differential equations (17) and (21) are investigated. For the treatment of nonlinear differential equations with time-dependent coefficients, Lyapunov introduced the concept of characteristic numbers.

We now define [16,17] the spectrum of Lyapunov exponents in the manner most relevant to the spectral calculations. Given a continuous dynamical system in an n-dimensional phase space, we monitor the long-term evolution of an infinitesimal n-sphere of initial conditions; the sphere will become an n-ellipsoid due to the locally deforming nature of the flow. The ith one-dimensional Lyapunov exponents is then defined in terms of the length of the ellipsoidal principal axis $p_i(t)$:

$$LE_i = \lim_{t\to\infty} \frac{1}{t} \log_2 \frac{p_i(t)}{p_i(0)} \tag{23}$$

where the LE_i are ordered from the largest to the smallest. Thus the Lyapunov exponents are related to the expanding or contracting nature of different directions in phase space.

The sign of Lyapunov exponents determines whether or not the unperturbed motion is stable [18]. According to Lyapunov, if all the exponents are negative then the unperturbed motion is asymptotically stable. In addition, Chetaev [19,20] showed that if one of the Lyapunov exponents is positive then the unperturbed motion is unstable.

Since the phase space volume shrinks to zero for a dissipative system, the stable, steady-state motion for an N-dimensional system lie on a "surface" of dimension less than N. Loosely speaking, this surface is called an attractor. There are four types of attractors in dynamic systems: fixed-point,

limit cycles, tori, and chaotic attractors. An attractor which consist of only one state is called a "fixed-point", it is a "steady state" for the system — once the system is close to that state, it enters that state; and once the system is in that state, it does not leave. Limit cycles represent periodic motions, tori represent quasiperiodic motions. Chaotic attractors are crucial to dissipative dynamical systems that are aperiodic. Fixed-point, limit cycles manifest regularity, chaotic attractors tend to appear highly irregular. It is worth noting that fixed-point attractors, limit cycles and tori are predictable, chaotic attractors exhibit unpredictable and bizarre motions. In a chaotic attractor, orbits of nearby points must diverge from each other due to the sensitive dependence on initial condition. If you make even the slightest change in the initial configuration of the system, then the resulting behavior of the system may be dramatically different. The dimension of the attractor reflects one of the essential aspects of dissipative dynamics; that is, the contraction of the phase volume. The dimension of an equilibrium point is zero and that of a limit cycle is one. But since a chaotic attractor is generated by contraction accompanied with stretching and folding of the state trajectories, it has a different dimension that may not be defined by an integer number. The Lyapunov spectrum is closely related to the fractional dimension of the associated strange attractor. The main purpose of the Lyapunov exponents is to characterize the dynamical properties of orbits and trajectories on attractors, the fractal dimension focuses on the geometry of attractor. Lyapunov characteristic exponents show the rate of exponential divergence or convergence of nearby trajectories from the chaotic attractor according to whether they are positive or negative, respectively. The concept of "fractal dimension" provides a second important tool, by means of which we can attempt to give a quantitative characterization of chaotic attractors. The fractal dimension is a measure of the extent to which orbits fill a certain subspace, and a noninteger dimension is a hallmark of a strange attractor. A noninteger fractal dimension indicates that orbits of a system tend to fill up less than an integer subspace of the phase space. A trajectory of a dynamical system with exponents all negative corresponds to a fixed point. A limit cycle, on the other hand, has one zero exponent, the rest being negative. An attractor for a dissipative system with one or more positive Lyapunov exponents is said to be "strange" or "chaotic.

For calculating the exponents the method suggested by Wolf et al. is used [17]. To compute the fractal dimension of the strange attractor we use the equation given by Frederickson et al. [21]

$$D_0 = j + \frac{\sum_{i=1}^{j} LE_i}{|LE_{j+1}|}. \tag{24}$$

j is defined by the condition

$$\sum_{i=1}^{j} LE_i > 0 \quad \text{and} \quad \sum_{i=1}^{j+1} LE_i < 0. \tag{25}$$

4. Numerical analysis and discussion

Letting $x_1 = f$, $x_4 = t$, Eq. (17) is reduced to a system of first-order equations

$$\dot{x}_1 = x_2,$$

$$\dot{x}_2 = x_3,$$

$$\dot{x}_3 = R_1 x_1 + R_2 x_2 - \alpha x_3 - 3q_1 q_3 x_1^2 x_2 + q_1 q_2 q_3 \mathrm{e}^{-\alpha x_4} x_2 Z + R_3 x_1^3, \tag{26}$$

$$\dot{x}_4 = 1,$$

where

$$R_1 = -\alpha\Omega^2[1 - 2\eta\cos(\theta x_4)] - 2\eta\theta\Omega^2 \sin\theta x_4 + q_2 q_3,$$
$$R_2 = -\Omega^2[1 - 2\eta\cos(\theta x_4)], \quad R_3 = -\alpha q_1 q_3 + q_1 q_2 q_3. \tag{27}$$

The trapezoidal rule can be used to compute the integration Z, i.e., when $t = k\Delta t$ (k is integer and larger than 1, Δt is time incremental)

$$Z = \int_0^t \mathrm{e}^{\alpha\tau} f^2 \,\mathrm{d}\tau = SJF + \frac{\Delta t}{2}\mathrm{e}^{\alpha(k-1)\Delta t} f_{k-1}^2 + \frac{\Delta t}{2}\mathrm{e}^{\alpha k\Delta t} f_k^2, \tag{28}$$

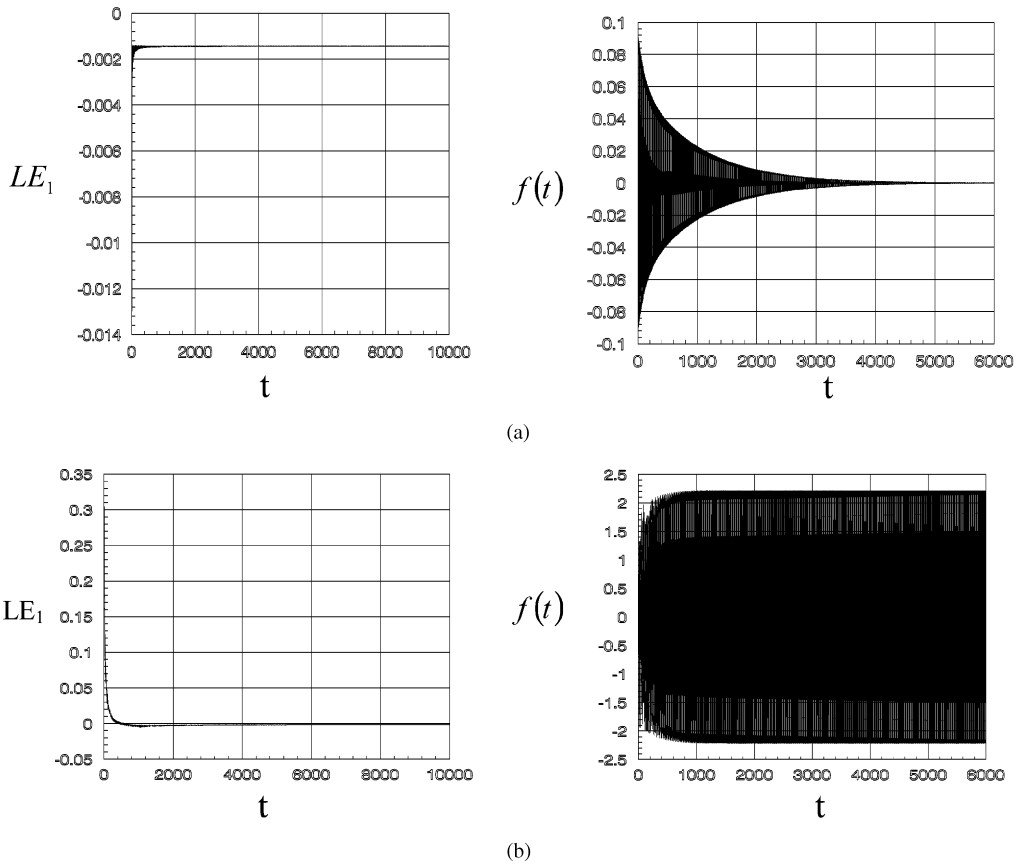

Fig. 2. The largest Lyapunov exponents LE_1 and the deflection $f(t)$ for $\alpha = 0.01$, $\omega = 1$, $l/h = 50$, $\eta_c = 9 \times 10^{-3}$ and (a) $\eta = 0.007$, (b) $\eta = 0.5$.

where

$$f_k = f|_{t=k\Delta t}, \quad SJF = \sum_{i=2}^{k} \frac{\Delta t}{2}[e^{\alpha(i-2)\Delta t} f_{i-2}^2 + e^{\alpha(i-1)\Delta t} f_{i-1}^2]. \tag{29}$$

Similarly, let $x_1 = f$, $x_4 = t$ Eq. (21) is reduced to a system of first-order equations of the form:

$$\begin{aligned} \dot{x}_1 &= x_2, \\ \dot{x}_2 &= x_3, \\ \dot{x}_3 &= R_4 x_1 + R_2 x_2 - \alpha x_3, \\ \dot{x}_4 &= 1, \end{aligned} \tag{30}$$

where

$$R_4 = -\alpha\Omega^2[1 - 2\eta\cos(\theta x_4)] - 2\eta\theta\Omega^2 \sin\theta x_4 + q_2 q_3 \tag{31}$$

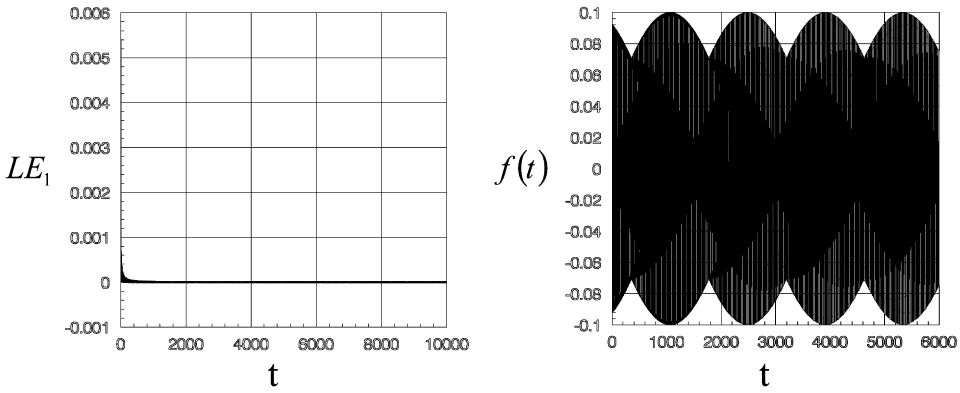

(a)

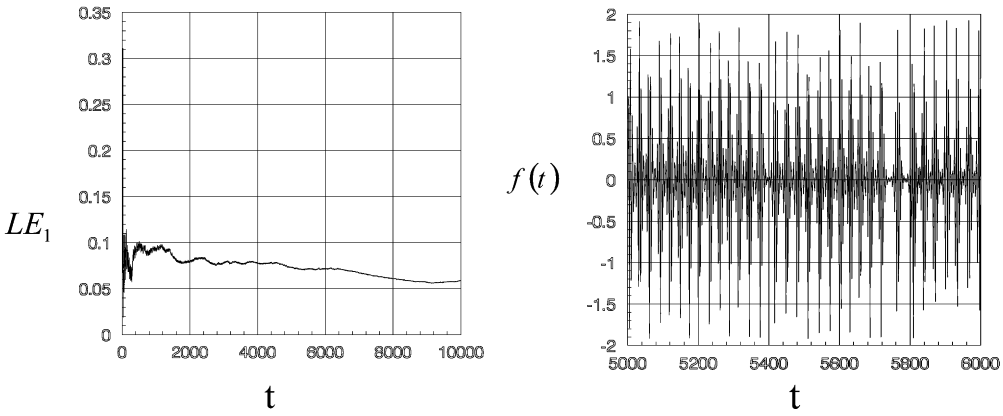

(b)

Fig. 3. The largest Lyapunov exponents LE_1 and the deflection $f(t)$ for $\alpha = 0.000001$, $\omega = 1$, $l/h = 50$, $\eta_c = 9 \times 10^{-7}$ and (a) $\eta = 0.0000007$, (b) $\eta = 0.5$

The numerical results were obtained by using $Y(t) = A + B\mathrm{e}^{-\alpha t} = 0.1 + 0.9\mathrm{e}^{-\alpha t}$, $\mu = 0.46$, $N_{xs} = 0$, $\Omega = \omega$ and $\theta = 2\omega$.

The numerical time integrations of Eqs. (26) and (30) are conducted using the fourth-order Runge–Kutta method with step size $\Delta t = (2\pi/\theta)/200$. An algorithm due to Wolf et al. [17] is used to calculate the Lyapunov exponents numerically. In this paper, the initial conditions are $f(0) = 0.1$, $\dot{f}(0) = 0$, the value of $\ddot{f}(0)$ is obtained by introducing $t = 0$ and $f(0) = 0.1$ in Eqs. (15) and (20).

The numerical results are shown in Figs. 2–7, where, Figs. 5 and 6 are solution of linear analysis, others are nonlinear solutions.

In Fig. 2a, $LE_1 = -1.4454 \times 10^{-3}, LE_2 = -1.4965 \times 10^{-3}, LE_3 = -1.1485 \times 10^{-2}, LE_t = 0$. The signs of LE_1, LE_2 and LE_3 are $(-,-,-)$, so, the unperturbed motion is asymptotically stable. The attractor is a stable fixed point.

In Fig. 2b, $LE_1 = -1.5927 \times 10^{-3} \approx 0$, $LE_2 = -6.2646 \times 10^{-3}$, $LE_3 = -6.5697 \times 10^{-3}$, $LE_t = 0$. The signs of LE_1, LE_2 and LE_3 are $(0,-,-)$. The attractor is a limit cycle.

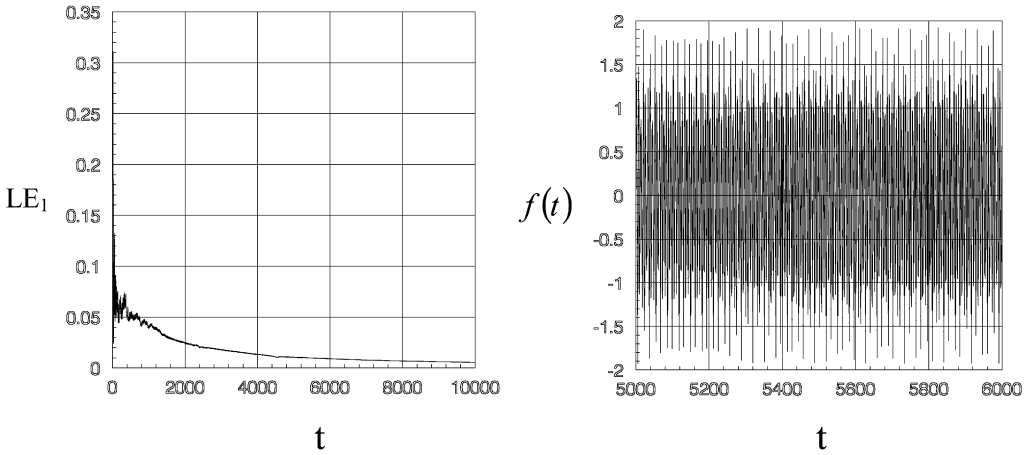

Fig. 4. The largest Lyapunov exponents LE_1 and the deflection $f(t)$ for $\alpha = 0.0001$, $\omega = 1$, $l/h = 50$, $\eta_c = 9 \times 10^{-5}$, $\eta = 0.5$.

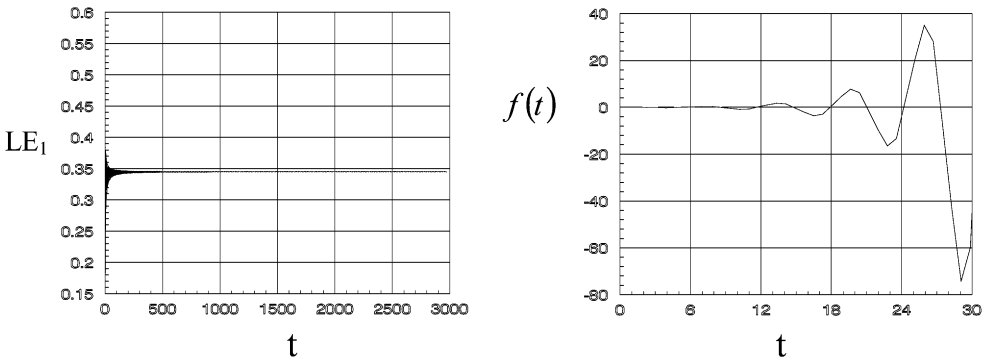

Fig. 5. The largest Lyapunov exponents LE_1 and the deflection $f(t)$ for $\alpha = 0.01$, $\omega = 1$, $l/h = 50$, $\eta_c = 9 \times 10^{-3}$, for linear analysis, $\eta = 0.5$.

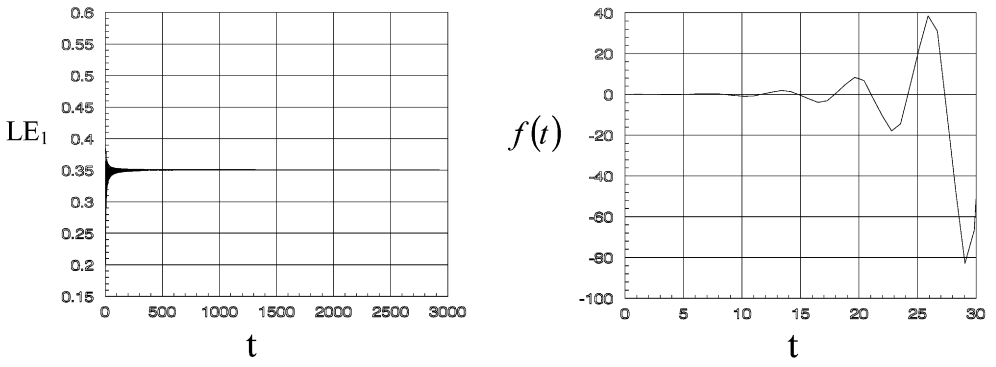

Fig. 6. The largest Lyapunov exponents LE_1 and the deflection $f(t)$ for $\alpha = 0.000001$, $\omega = 1$, $l/h = 50$, $\eta_c = 9 \times 10^{-7}$, for linear analysis, $\eta = 0.5$.

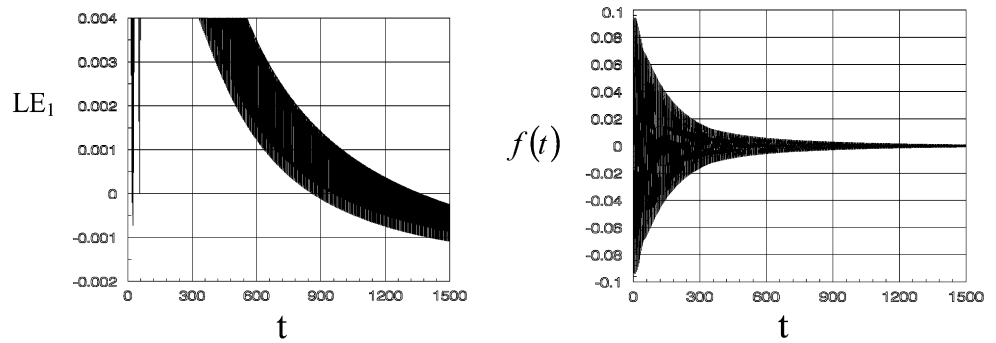

Fig. 7. The largest Lyapunov exponents LE_1 and the deflection $f(t)$ for $\alpha = 0.01$, $\omega = 25$, $l/h = 10$, $\eta_c = 3.6 \times 10^{-4}$, $\eta = 0.0002$.

In Fig. 3a, $LE_1 = 1.3557 \times 10^{-5} \approx 0$, $LE_2 = -9.4272 \times 10^{-7}$, $LE_3 = -1.4057 \times 10^{-5}$, $LE_t = 0$. The signs of LE_1, LE_2 and LE_3 are $(0, -, -)$, The attractor is a limit cycle.

In Fig. 3b, $LE_1 = 5.7807 \times 10^{-2}$, $LE_2 = 6.3256 \times 10^{-4} \approx 0$, $LE_3 = -5.8441 \times 10^{-2}$, $LE_t = 0$. The signs of LE_1, LE_2 and LE_3 are $(+, 0, -)$. There exist chaotic attractor. Using Eq. (24), the fractal dimensions of the strange attractor of the system is found to be

$$D_0 = j + \frac{\sum_{i=1}^{j} LE_i}{|LE_{j+1}|} = 3 + \frac{5.7807 \times 10^{-2}}{5.8441 \times 10^{-2}} = 3.989.$$

In Fig. 4, $LE_1 = 4.7602 \times 10^{-3}, LE_2 = 5.8916 \times 10^{-4} \approx 0, LE_3 = -5.4937 \times 10^{-3}$, $LE_t = 0$. The signs of LE_1, LE_2 and LE_3 are $(+, 0, -)$. There exist chaotic attractor. Using relation Eq. (24), the fractal dimensions of the strange attractor of the system is found to be

$$D_0 = j + \frac{\sum_{i=1}^{j} LE_i}{|LE_{j+1}|} = 3 + \frac{4.7602 \times 10^{-3}}{5.4937 \times 10^{-3}} = 3.866.$$

In Fig. 5, $LE_1 = 3.451 \times 10^{-1}$, $LE_2 = -5.8178 \times 10^{-3}$, $LE_3 = -3.5368 \times 10^{-1}$, $LE_t = 0$.

In Fig. 6, $LE_1 = 3.5062 \times 10^{-1}$, $LE_2 = -7.0996 \times 10^{-3}$, $LE_3 = -3.4352 \times 10^{-1}$, $LE_t = 0$.

In above two cases (Figs. 5 and 6), because the analyses are based on the small deflections theory (geometrically linear analysis), there exists no chaotic attractor. Whereas, for $LE_1 > 0$ the systems are unstable.

In Fig. 7, $LE_1 = -1.4254 \times 10^{-3}$, $LE_2 = -2.9466 \times 10^{-3}$, $LE_3 = -1.0055 \times 10^{-2}$, $LE_t = 0$. The signs of LE_1, LE_2 and LE_3 are $(-,-,-)$, so, the unperturbed motion is asymptotically stable. The attractor is a stable fixed point.

5. Conclusions

1. Because of the stretching of the middle plane, the response amplitude within the large deflections theory is smaller than that predicted by using the small deflections theory (cf. Figs. 2b to 5; Figs. 3b to 6).
2. When $\eta < \eta_c$, the system is asymptotically stable regardless of the values of the viscoelastic parameters (see Figs. 2a and 7) so long as $\alpha = 1/t_r$ is not very small (see Fig. 3a).
3. An unstable system may become stable at larger values of α (see Figs. 2b and 3b). And from Eq. (22), at large α, η_c is increased, so that α also stabilizes the system.
4. Due to the geometry nonlinearity, there may exist chaotic attractor in the dynamical system for a particular set of parameters (see Figs. 3b and 4).

Acknowledgements

This work was supported by the Chinese National Natural Science Foundation.

References

[1] Bolotin VV. The dynamic stability of elastic systems [Translated by Weingarten VI et al.]. San Francisco: Holden-Day, 1964.
[2] Evan-Iwanowski RM. On the parametric response of structures. Applied Mechanics Reviews 1965;18:699–702.
[3] Evan-Iwanowski RM. Resonant oscillations in mechanical systems. Amsterdam: Elsevier, 1976.
[4] Aboudi J, Cederbaum G, Elishakoff I. Dynamic stability analysis of viscoelastic plates by Lyapunov exponents. Journal of Sound and Vibration 1990;139(3):459–67.
[5] Touati D, Cederbaum G. Dynamic stability of nonlinear viscoelastic plates. International Journal of Solids and Structures 1994;31(17):2367–76.
[6] Cederbaum G, Aboudi J, Elishakoff I. Dynamic instability of shear-deformable viscoelastic laminated plates by Lyapunov exponents. International Journal of Solids and Structures 1991;28(3):317–27.
[7] Cederbaum G, Mond M. Stability properties of a viscoelastic column under a periodic force. Journal of Applied Mechanics 1992;59:16–9.
[8] Cederbaum G. Parametric excitation of viscoelastic plates. Mechanisms of Structural Mechanics 1992;20: 37–51.
[9] Cederbaum G. Dynamic instability of viscoelastic orthotropic laminated plates. Composite Structures 1991;19:131–44.

[10] Badalov FB, Eshmatov Kh, Akbarov UI. Stability of a viscoelastic plate under dynamic loading. Soviet Applied Mechanics [Translated from Prikladnaya Mekhanika] 1991;27(9):892–9.
[11] Zhu Yuanyuan, Cheng Changjun. Stability analysis of viscoelastic rectangular plates. Acta Mechanica Solida Sinica 1996;17(3):257–62 [in Chinese].
[12] Touati D, Cederbaum G. Influence of large deflections on the dynamic stability of nonlinear viscoelastic plates. Acta Mechanica 1995;113:215–31.
[13] Schapery RA. Viscoelastic behavior and analysis of composite materials. In: Sendeckyj GP, editor. Composite materials, vol. 2. New York: Academic Press, 1974.
[14] Vol'mir AS. Nonlinear dynamics of plates and shells. Moscow: Nauka, 1972 [in Russian].
[15] McLachlan NW. Theory and application of Mathieu functions. New York: Dover, 1964.
[16] Benettin G, Galgani L, Giorgilli A, Strelcyn J-M. Lyapunov characteristic exponents for smooth dynamical systems and for hamiltonian system; a method for computing all of them. Meccanica 1980;15:9–20.
[17] Alan W, Jack BS, Harry LS, John AV. Determining Lyapunov exponents from a time series. Physica 1985;16D:285–317.
[18] Hahn W. Stability of motion. Berlin: Springer, 1967.
[19] Chetaev NG. On certain questions related to the problem of stability of unsteady motion. Journal of Applied Mathematics and Mechanics 1960;24(1):6–22.
[20] Chetaev NG. Stability of motion [Oxford Translation from 2nd Russian revised edn]. Oxford: Pergamon Press, 1961.
[21] Frederickson P, Kaplan J, Yorke E, Yorke J. The Lyapunov dimension of strange attractors. Journal of Differential Equations 1983;49:185.